Human Molecular Genetics, 2003, Vol. 12, No. 24 **3215–3223**
DOI: 10.1093/hmg/ddg358

PCDH15 is expressed in the neurosensory epithelium of the eye and ear and mutant alleles are responsible for both USH1F and DFNB23

Zubair M. Ahmed[1,4], Saima Riazuddin[1], Jamil Ahmad[4], Steve L. Bernstein[5], Yan Guo[5], Muhammad F. Sabar[4], Paul Sieving[6], Sheikh Riazuddin[4], Andrew J. Griffith[2,3], Thomas B. Friedman[1], Inna A. Belyantseva[1] and Edward R. Wilcox[1,*]

[1]Section on Human Genetics, [2]Section on Gene Structure and Function, Laboratory of Molecular Genetics, and [3]Hearing Section, National Institute on Deafness and Other Communication Disorders, National Institutes of Health, Rockville, MD, USA, [4]National Center of Excellence in Molecular Biology, Punjab University, Lahore, Pakistan, [5]Department of Ophthalmology, University of Maryland School of Medicine, Baltimore, MD, USA and [6]National Eye Institute, National Institutes of Health, Bethesda, MD, USA

Received June 27, 2003; Revised and Accepted October 17, 2003 DDBJ/EMBL/GenBank accession no.[†]

Recessive splice site and nonsense mutations of *PCDH15*, encoding protocadherin 15, are known to cause deafness and retinitis pigmentosa in Usher syndrome type 1F (USH1F). Here we report that non-syndromic recessive hearing loss (DFNB23) is caused by missense mutations of *PCDH15.* This suggests a genotype–phenotype correlation in which hypomorphic alleles cause non-syndromic hearing loss, while more severe mutations of this gene result in USH1F. We localized protocadherin 15 to inner ear hair cell stereocilia, and to retinal photoreceptors by immunocytochemistry. Our results further strengthen the importance of protocadherin 15 in the morphogenesis and cohesion of stereocilia bundles and retinal photoreceptor cell maintenance or function.

INTRODUCTION

Usher syndrome type 1 (USH1; OMIM 602083) is a hereditary neurosensory disorder characterized by profound congenital deafness, vestibular areflexia and retinitis pigmentosa (1,2). Seven USH1 loci have been mapped and genes for five of them have been identified: USH1B (*MYO7A*), USH1C (*USH1C*), USH1D (*CDH23*), USH1F (*PCDH15*) and USH1G (*SANS*) (3–10). These genes encode unconventional myosin VIIA, harmonin, cadherin 23, protocadherin 15 and SANS, respectively (3–10). Although most of the mutant alleles of these genes are associated with Usher syndrome, some missense mutations of *USH1C* and *CDH23* are associated with non-syndromic hearing loss (6,11,12).

To date, all of the reported mutations of *PCDH15* on chromosome 10q21.1 cause Usher syndrome (3,4,13). *PCDH15* belongs to the cadherin superfamily of calcium-dependent cell–cell adhesion molecules (3). Protocadherins represent a large family of non-classical cadherins that are structurally and functionally divergent from the classic cadherins (14). In higher vertebrates, protocadherins are thought to be involved in a variety of functions, including neural circuit formation and synapse formation (15).

In Ames waltzer (*av*) mice, recessive mutations of *Pcdh15* cause deafness with disorganized stereocilia bundles and degeneration of inner ear neuroepithelia (16–19). This phenotype is shared with all of the known mouse strains segregating mutant alleles of USH1 orthologs: shaker-1 (*sh1*), waltzer (*v*) and jackson shaker (*js*), the mouse models for Usher syndrome type 1B, 1D and 1G, respectively (20–22). Recently, it has been shown that myosin VIIa, harmonin and cadherin 23 co-localize in the stereocilia of hair cells, and can interact with each other *in vitro* and in heterologous expression systems (23,24). It has been proposed that these proteins may form a complex essential for cohesiveness of the stereocilia bundle (23,24), raising the possibility that similar interactions may also occur in the eye. Myosin VIIa, harmonin and cadherin 23 are expressed in photoreceptor cells of mouse retina, whereas myosin VIIa is

*To whom correspondence should be addressed at: 5 Research Court, 2A-19, Rockville, MD 20850, USA. Tel: +1 3014024162; Fax: +1 3014808019; Email: wilcoxe@nidcd.nih.gov
[†]*PCDH15* isoform B reported in this manuscript has been deposited in NCBI GenBank and the accession number is AY388963.

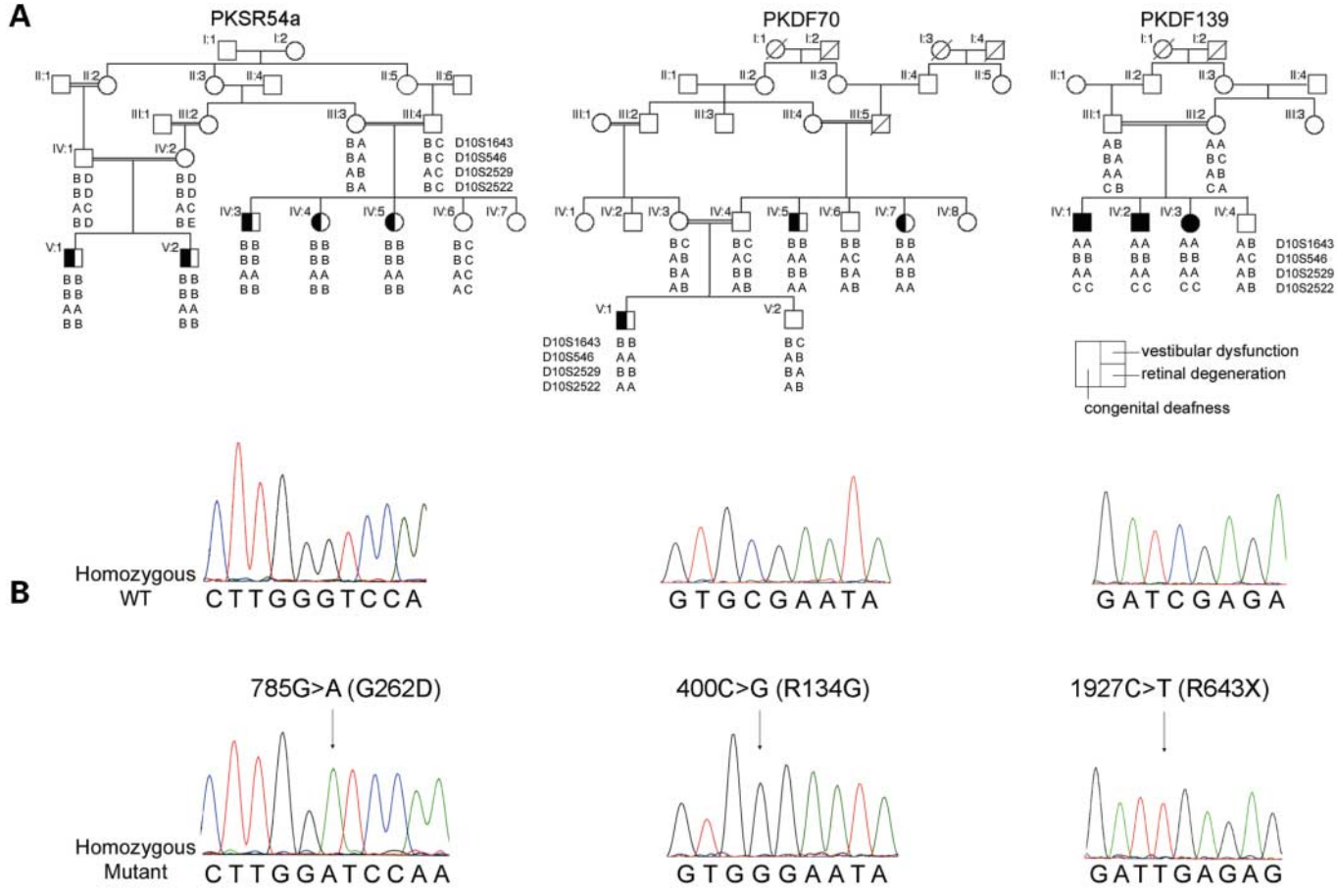

Figure 1. DFNB23 and USH1F families with *PCDH15* mutations. (**A**) Pedigrees of families segregating non-syndromic recessive deafness DFNB23 and Usher syndrome type 1F with their haplotypes for markers on chromosome 10. Each family has a different *PCDH15*-linked haplotype (**B**) PKSR54a-electropherograms of amplimers from genomic DNA templates illustrate homozygosity for a 785G > A transition mutation (G262D, exon 8) in an affected individual and homozygosity for the wild-type allele in an unaffected individual. PKDF-70-electropherograms illustrating genotypes of a homozygous wild-type allele and a person homozygous for 400C > G transverion mutation. PKDF-139-electropherograms of the transition mutation 1927C > T and the wild-type allele are shown.

also expressed in the apical processes of retinal pigmented epithelium (RPE) (7,24–27). Although myosin VIIa appears to be present in connecting cilium of photoreceptors, the subcellular locations of harmonin, cadherin 23 and SANS in photoreceptors are unknown (24,26,27). Interestingly, the mouse models of cadherin 23, protocadherin 15 and SANS mutations do not have any reported retinal phenotype, which may reflect interspecies differences in the functional requirements for these proteins or functional redundancy with other proteins in the retina. We thus sought to address the molecular genetic and cell biological bases for these observations of protocadherin 15 function and its associated mutant pathologies in the eye and ear.

RESULTS

Mutant alleles of *PCDH15* are associated with nonsyndromic recessive deafness

We screened DNA samples from ~400 families with recessive prelingual hearing loss with short tandem repeat (STR) markers closely linked to *PCDH15* (3) to test the hypothesis that there are mutant alleles of *PCDH15* associated with non-syndromic deafness. Recessive deafness in three families (PKSR54a, PKDF70 and PKDF139; Fig. 1A) co-segregated with STR markers linked to *PCDH15* (Table 1). Pure-tone air conduction audiometry showed severe to profound sensorineural hearing loss segregating in family PKSR54a and profound deafness in families PKDF70 and PKDF139. Families PKSR54a and PKDF70 have no history of nyctalopia, and the funduscopy and electroretinograms (ERGs) were normal in two older affected individuals (Fig. 2) from each family (age range 13–44 years). Electronystagmography (ENG) with caloric stimulation

Table 1. Two-point LOD scores (at $\theta = 0$)

Marker	LOD scores for family		
	PKSR54a	PKDF70	PKDF139
D10S1643	3.49	0.98	1.86
D10S546	3.97	3.26	2.20
D10S2529	2.28	1.99	1.78
D10S2522	4.11	2.98	2.31

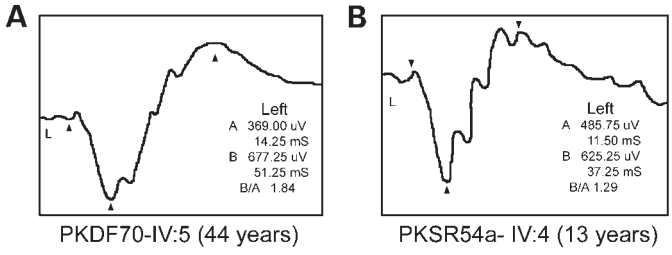

Figure 2. Electroretinograms of left eyes for individuals IV:5 from family PKDF70 and IV:4 from PKSR54a. Both hearing-impaired individuals have normal *A*- and *B*-wave amplitudes as well as *B*/*A* ratios. Electroretinograms from the right eye of each of these individuals were identical to those obtained from their left eyes (data not shown).

revealed intact vestibular response in these affected individuals. Thus families PKSR54a and PKDF70 have non-syndromic recessive deafness (DFNB23; Hereditary Hearing Loss homepage), whereas similar evaluations of older affected individuals (aged 6 and 9 years) from family PKDF139 revealed clinical features typical of Usher syndrome type 1, confirming that our clinical tests for RP are sensitive. The three affected members of family PKDF139 with USH1 were homozygous for 1927C > T (Fig. 1B), which introduces a stop codon (R643X) in exon 16 of *PCDH15* (Fig. 3A and B). This mutation was not found in 200 chromosomes from ethnically matched control DNA samples from Pakistan.

Sequence analysis of all *PCDH15* exons (Fig. 3A) in affected members of family PKSR54a demonstrated homozygosity for a missense mutation (785G > A, G262D; Fig. 1B) in exon 8, which encodes part of the second of 11 extracellular cadherin domains (EC) of protocadherin 15 (Fig. 3B). In family PKDF70, affected individuals are homozygous for a transversion mutation (400C > G, R134G; Fig. 1B) in exon 5 (Fig. 3A), which encodes part of the first EC domain (Fig. 3B). These two mutations were not found in 150 ethnically matched control DNA samples from Pakistan. A ClustalW alignment showed conservation of the R134 and G262 residues among the protocadherin 15 orthologs from mouse, rat, zebrafish and puffer fish (data not shown).

Previous studies showed abundant expression of a 3.5 kb *PCDH15* transcript in human retina (3). Through the combination of conserved synteny between human and mouse genome and 5′ RACE on retina cDNA, we cloned the shorter isoform of *PCDH15* (Fig. 3A). The start codon of this isoform (named as *PCDH15* isoform B) is found in the middle of the exon 25b (Fig. 3A) at 374 bp (GenBank accession number AY388963). The three mutations herein reported are present in exons upstream from transcription start site for *PCDH15* isoform B.

Protocadherin 15 is expressed in sensory epithelia of the eye and ear

In order to characterize the cellular localization of protocadherin 15 with immunofluorescent confocal microscopy, we produced rabbit polyclonal antiserum (PB303) against a synthetic peptide immunogen from part of the cytoplasmic domain of mouse protocadherin 15 encoded by exon 33. Western blot analysis of this serum (PB303) on protein extracts from adult C57BL/6 mouse brain, retina, liver, spleen and cochlear homogenates (50 μg/lane) showed two bands corresponding to the proteins of the predicted sizes for protocadherin 15 isoforms (180 and 60 kDa, respectively; Fig. 3A and C). Immunoflourescent staining with PB303 antibody overlapped with the signal produced by tagged cytoplasmic domain of protocadherin 15 expressed in lymphoblast cells, which lack endogenous expression of protocadherin 15 (Fig. 3D–G). These findings confirm the specificity of the antibody for protocadherin 15.

Western blot analysis also revealed the expression of protocadherin 15 in the mouse retina (Fig. 3C). To explore the precise cellular localization of protocadherin 15 in the eye, human (Fig. 4A and B) and monkey (Fig. 4C and D) retinae were examined for immunoreactivity with PB303. Strong protocadherin 15 immunoreactivity is present in the photoreceptors, particularly in the outer photoreceptor segments (Fig. 4A and B). Strong protocadherin 15 immunoreactivity is apparent in cones, which are more obvious in frozen sections of monkey retina (Fig. 4C; arrowheads). Rod photoreceptors also showed diffuse positive signal throughout the photoreceptor layer (Fig. 4C; arrows).

Protocadherin 15 immunoreactivity was also detected in C57BL/6 mouse organ of Corti and vestibular hair cells (Fig. 5). The immunoreactivity was seen along the length of stereocilia (Fig. 5B and C), in the cuticular plate (Fig. 5E and F), and diffusely distributed in the cytoplasm of inner and outer hair cells (data not shown). A similar pattern was observed in vestibular hair cells of cristae ampullaris (Fig. 5H and I), utricular (Fig. 5K and L) and saccular maculae (data not shown). The amount of protocadherin 15 immunoreactivity in the stereocilia appears to vary among different hair bundles and among stereocilia of different lengths in the same hair bundle. The specific immunofluorescent signal was generally stronger in longer stereocilia (Fig. 5H and K; arrows), compared with shorter ones within the same bundle of a vestibular hair cell (Fig. 5H and K; arrow heads). No protocadherin 15 immunoreactivity was observed in the kinocilium of developing cochlear and vestibular hair cells as revealed by simultaneous staining with anti-tubulin antibody (data not shown). We also studied the subcellular distribution of protocadherin 15 during the period of auditory hair bundle differentiation (E16–P21) in the mouse. Protocadherin 15 was detected along the entire stereocilia length as soon as stereocilia become distinguishable among the microvilli at the apical surface of organ of Corti hair cells.

DISCUSSION

Here we have demonstrated that *PCDH15* mutant alleles can cause either Usher syndrome type 1 (USH1F) (3,13) or non-syndromic hearing loss (DFNB23). Our data suggest a genotype–phenotype correlation in which hypomorphic alleles are associated with non-syndromic hearing loss, while more severe mutations of this gene result in USH1. Similar correlations have been demonstrated for *USH1C* and *CDH23* (6,11,12,28), indicating the residual function associated with some missense allele products is sufficient for normal vision but not for hearing.

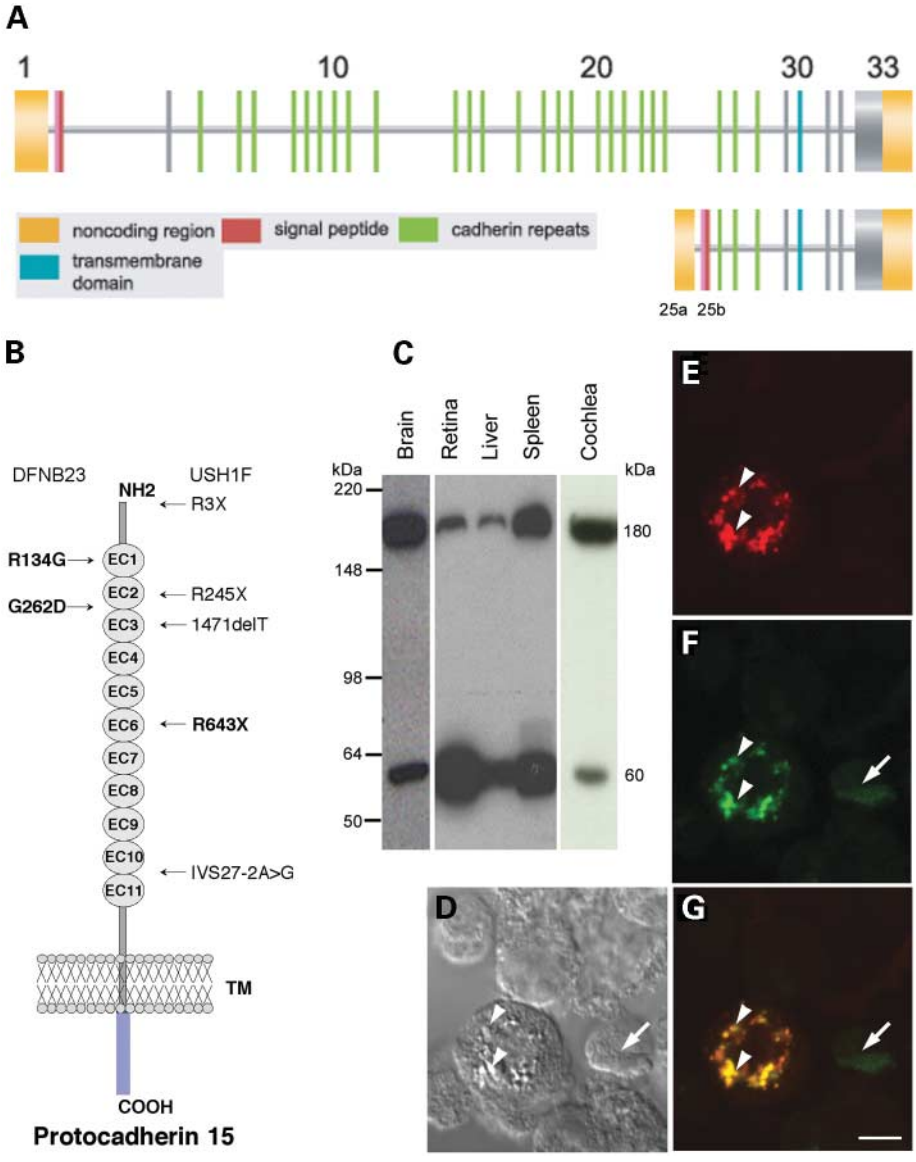

Figure 3. Predicted protocadherin 15 structure and a western blot using the anti-Pcdh15 antiserum (PB303). (**A**) Structure of *PCDH15* isoforms encoding 180 and 60 kDa proteins. Newly identified isoform B has two unique exons (25a and 25b) encoding the 5′-UTR and transcription start site, respectively. Isoform B shares 8 exons (26–33) with the previously reported 7.0 kb isoform. (**B**) An illustration of isoform A of protocadherin 15 showing the predicted structural motifs along with the mutations causing DFNB23 (left) and USH1F (right) in humans (3,4,13). The three mutant alleles reported in this study are highlighted in bold. Shown in blue is the region of cytoplasmic domain of protocadherin 15 tagged with HcRed1 for transfection studies shown in panel D to G. TM, transmembrane domain; EC, extracellular cadherin domain. (**C**) Western analysis, using anti-Pcdh15 antibody (PB303) and protein extracts from adult C57BL/6 mouse brain, retina, liver, spleen and cochlea homogenates (50 µg/lane), showed two bands corresponding to the proteins of the predicted sizes for protocadherin 15 isoforms (180 and 60 kDa). Neither protein band was detected when the antibody was incubated with an excess of the immunogenic peptide prior to immunoblotting (data not shown). (**D**) Nomarski image of cultured lymphoblast cells transfected with tagged cytoplamic domain of *Pcdh15*. The arrow and arrowheads indicate the cell regions corresponding to a specific fluorescence staining shown in panels E–G. (**E**–**G**) Immunofluorescence images of lymphoblast cells transfected with HcRed1 tagged cytoplasmic region of protocadherin 15 (E, red channel) and stained with PB303 antibody (F, green channel). (G) An overlay of red and green channels. PB303 antibody immunofluorescence overlapped with the signal produced by tagged cytoplasmic domain of protocadherin 15 expressed protein (arrowheads) reflecting the specificity of PB303 antibody for protocadherin 15. Non-transfected cells did not give staining with PB303 above the background level (arrow, F and G). Scale bar in G, 5 µm applied to panels D–G.

The clinical complexity of Usher syndrome reflects the high level of genetic heterogeneity, background and stochastic effects as well as shared structural features and physiological pathways in the cochlea and retina. The expression of protocadherin 15 in the organ of Corti (Fig. 5B, C, E and F) and in the vestibular apparatus (Fig. 5H, I, K and L) is consistent with the clinical outcome of USH1F subjects and *av* mice. The finding that protocadherin 15 staining is present in photoreceptor cells (Fig. 4) suggests that USH1F subjects are likely to have significant defects in color vision, and may have more frequent central visual complaints, night blindness and progressive peripheral vision loss, which is typical of rod

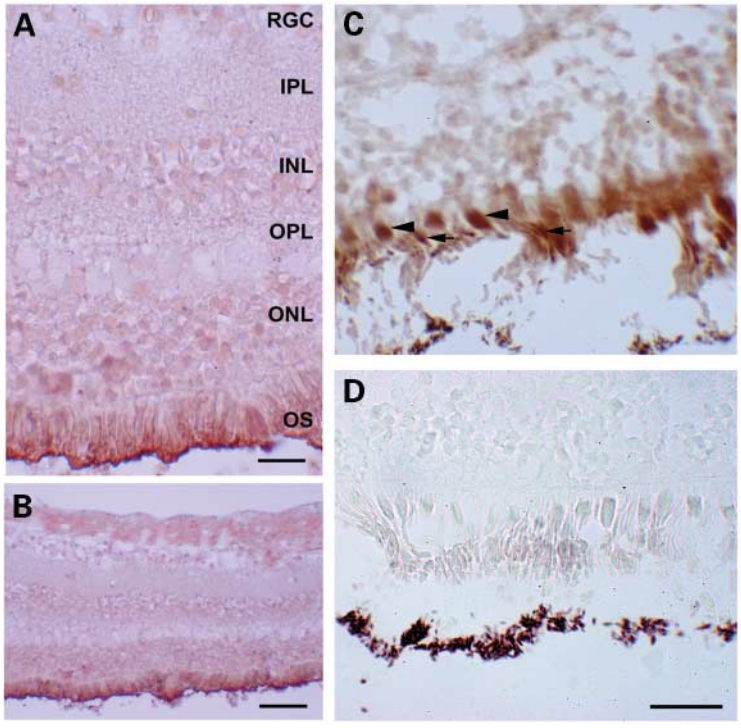

Figure 4. Expression of protocadherin 15 in the photoreceptor cells of human and monkey retina. Light background staining is present throughout all layers of the retina, but specific protocadherin 15 staining is localized to the photoreceptor cells (**A**–**C**). Protocadherin 15 immunoreactivity is present in the human photoreceptors, especially in the outer photoreceptor segments (A and B). Strong immunoreactivity is apparent in evenly spaced cone-shaped photoreceptors in frozen sections of monkey (macaque) retina (C; arrow heads). Rod photoreceptors are also positive, as shown by the diffuse positive signal throughout the photoreceptor layer (C; arrows). No immunoreactivity in photoreceptor cells is observed in the controls stained with secondary antibody. Dark brown granules present in the lower part of (**D**) are the melanin pigments from RPE. The scale bar is 20 μm in (A), (C) and (D) and 100 μm in (B). RGC, retinal ganglion cells; IPL, inner plexiform layer; INL, inner nuclear layer; OPL, outer plexiform layer; ONL, outer nuclear layer; OS, outer segment of rods and cones.

photoreceptor dysfunction. The clinical phenotype (progressive retinitis pigmentosa and tunnel vision) of older affected individuals (aged 6 and 9 years) of PKDF139 family are consistent with this expectation.

Hearing function depends upon the mechano-electrical transduction of auditory and vestibular stimuli which occur within polarized hair cell stereocilia bundles that are arranged in rows of increasing height (29). There are many different interconnections, including tip links, horizontal top connectors, lateral or shaft links and ankle links between adjacent stereocilia that are thought to help establish and maintain the integrity of the stereocilia bundles (30–32). Ankle links are present in mouse hair cell stereocilia up to P12 and then begin to disappear and are completely absent in adult mice (33). Harmonin isoform b and cadherin 23 are found in cochlear stereocilia during hair cell development, but not at P30 (23), raising the possibility that these proteins may be important for the development of stereocilia bundle and may have a role in the formation and maintenance of some transient links, such as ankle links, but not in the long-term maintenance of stereocilia bundle morphology. In contrast, lateral links are very fine strands that connect the membranes of adjacent stereocilia and are present along the length of the stereocilia even in adult mice (31,32). The developmental pattern and the distribution of protocadherin 15 in stereocilia of inner ear hair cells of adult mice (Fig. 5), taken together with the known function of protocadherins in cell adhesion, suggests that protocadherin 15 may have a role in the development and maintenance of these lateral links between stereocilia. The two missense mutations (R134G and G262D) associated with non-syndromic deafness are present in the first and second EC domains, respectively. We hypothesize that these missense mutations impair the ability of the EC domains to interact with each other to form the lateral links, hence destabilizing stereocilia bundles and causing deafness.

Our observation of protocadherin 15 staining in photoreceptors and retinal degeneration observed in USH1F individuals suggests that *PCDH15* is important for the maintenance or function of the photoreceptor cells. However, the two missense mutations that we found might not significantly impair the functional abilities of protocadherin 15 in the retina, hence DFNB23 individuals have normal vision. It is also possible that these mutations affect alternative transcripts, which are not necessary for retinal function in humans.

There is no reported retinal pathology in mice homozygous for truncating alleles of *Pcdh15* (36). This may reflect functional redundancy with other proteins in the retina or differences in other genetic, stochastic, and environmental factors such as light exposure. Elucidation of the causes of this dissimilarity could reveal molecular or cellular pathways for potential interventions to prevent or retard RP in USH1.

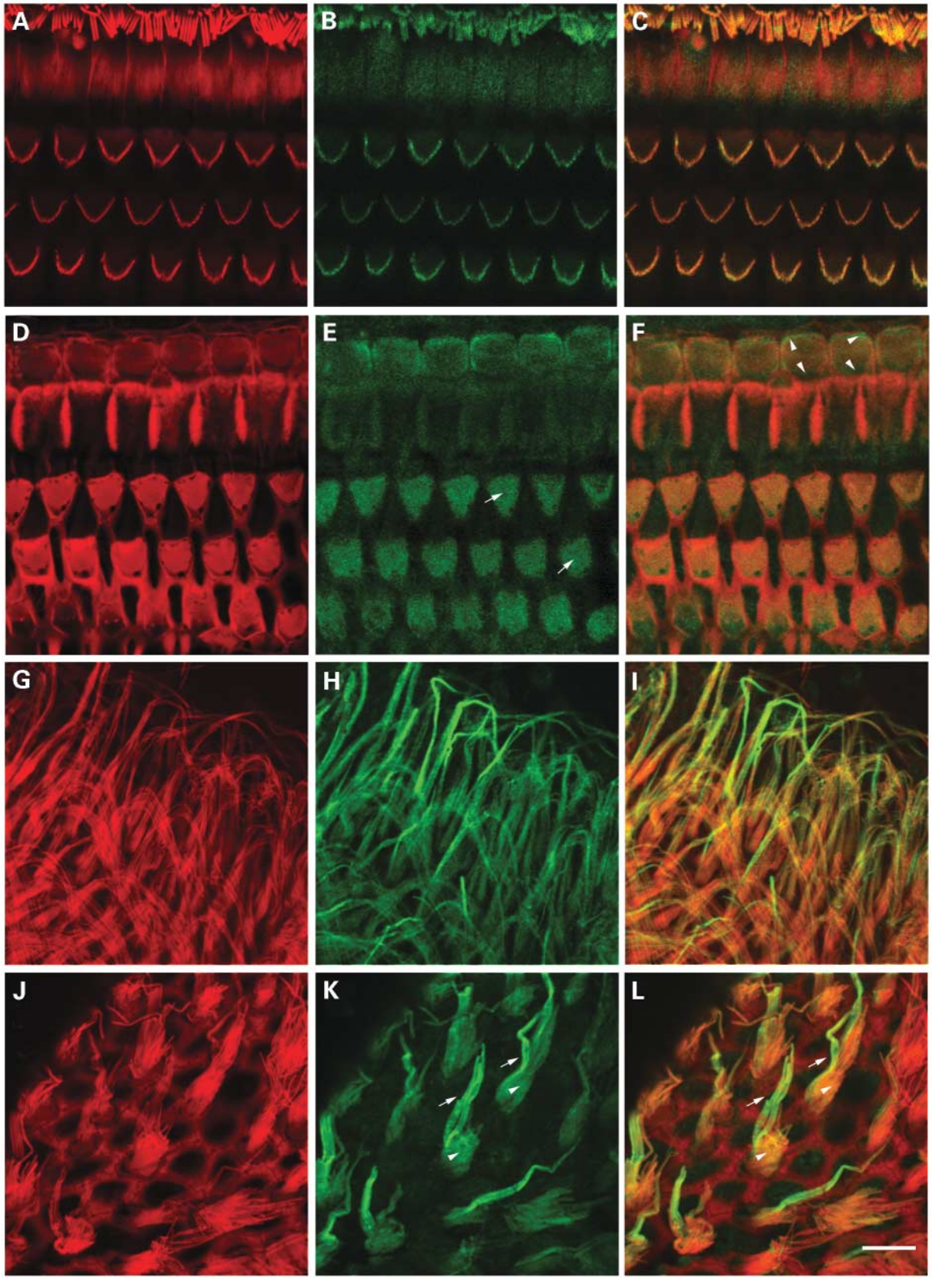

MATERIALS AND METHODS

Linkage and sequence analyses

Institutional review board approval (OH93-N-016) and written informed consent were obtained for all subjects in this study. To determine if affected members of these families have balance or ocular abnormalities, medical histories were taken with an emphasis on the vestibular and retinal phenotypes. Pure-tone audiometry, funduscopy or electroretinography (ERG) and electronystagmography (ENG) exams were performed on selected affected individuals from each family.

DNA was extracted from peripheral blood or buccal cells. DNA samples were PCR amplified using fluorescently labeled primers flanking polymorphic STR at USH1F. PCR products were visualized by gel electrophoresis on an ABI 377 DNA sequencer and genotypes determined using Genescan and Genotyper software (PE Applied Biosystems). The 33 coding and non-coding exons of *PCDH15* (Genbank accession number AY029237) in the participating members of families PKSR54a, PKDF70 and PKDF139 were PCR amplified and sequenced as described elsewhere (3).

LOD scores were calculated using FASTLINK (34). The disease was coded as fully penetrant and the disease allele frequency was set at 0.001. Meiotic recombination frequencies were assumed to be equal for males and females. The allele frequencies of the STRP markers were calculated by genotyping 96 random normal individuals from the same population.

Antibodies

Protocadherin 15 antiserum (PB303) was raised in rabbit against a synthetic peptide (CGAEPHRHPKGILRHVKNLAELEK; corresponding to residues 1860–1882 of the mouse sequence, Genbank accession number AAG53891). Amino acid residues used for antiserum production are 85% identical among mouse and human protocadherin 15. Antiserum was affinity purified (Pierce Biotechnology, Rockford, IL, USA) with the synthetic peptide used as the immunogen. Fluorescein-conjugated anti-rabbit IgG secondary antibody was obtained from Amersham Pharmacia Biotech (Arlington Heights, IL, USA).

Western blot analysis

C57BL/6 mouse brain, retina, liver and spleen were sonicated in an ice-cold protease inhibitor cocktail (Calbiochem Biosciences, La Jolla, CA, USA). Proteins were extracted and denatured by boiling for 5 min in SDS–PAGE sample buffer (0.125 M Tris–HCl, 20% glycerol, 4% SDS, 0.005% Bromophenol blue). A 50 μg protein sample was separated on a 4–20% gradient Tris–glycine gel (Novex, San Diego, CA, USA) and transferred to polyvinyldifluoride (PVDF) membranes, blocked overnight (O/N) with 5% dry milk in TBST (10 mM Tris–HCl pH 7.5, 150 mM NaCl, 0.05% Tween 20), and stained with anti-Pcdh15 antiserum (PB0303; 1 : 2000 in blocking solution) for 2 h at room temperature. After three washes the membranes were incubated in a 1 : 5000 dilution of horseradish peroxidase-conjugated anti-rabbit secondary antibody (Promega, Madison, WI, USA) for 30 min and developed using the ECL plus western blotting detection system (Amersham Pharmacia Biotech, Arlington Heights, IL, USA).

Expression construct

A cDNA encoding the cytoplasmic region of protocadherin 15 (AAG53891; amino acids 1403–1943) was obtained by PCR from a mouse (P0) retinal cDNA library. PCR product was subcloned into pHcRed1-C1 vector (Clontech, Palo Alto, CA, USA) for expression in lymphoblast cells, which, based on RT–PCR analysis, do not have endogenous expression of *PCDH15* (data not shown). Lymphoblast cells were cultured in 10% fetal bovine serum (FBS)-supplemented Dulbecco's modified Eagle's medium (DMEM). Transient transfection of these cells was performed using Lipofectamine-2000 reagent (Life Technologies, Gaithersburg, MD, USA). Fluorescence immunocytochemistry was carried out on fixed cells (4% PFA for 15 min). The staining procedure used was same as described below for the inner ear tissue.

Immunocytochemistry of mouse inner ear

Immunocytochemistry was performed as described previously (35). After 2 h fixation in 4% PFA, organ of Corti and vestibular organs were dissected in PBS at room temperature using a fine needle. Organ of Corti tissue samples were permeabilized in 0.5% Triton X-100 for 30 min and then washed in PBS. Non-specific binding sites were blocked using 5% normal goat serum (Life Technologies, Gaithersburg, MD, USA) and 2% bovine serum albumin (ICN, Aurora, OH, USA) in PBS. Samples were incubated for 2 h in the anti-Pcdh15 antisera (PB303) at a concentration of ~5 μg/ml in blocking solution. After three rinses in PBS, samples were incubated in a 1 : 200 dilution of the FITC conjugated anti-rabbit IgG secondary antibody for 30 min. After washing three times with PBS, samples were mounted using ProLong Antifade kit

Figure 5. Immunolocalization and confocal microscopy of protocadherin 15 in the organ of Corti and vestibular sensory epithelia. (**A**–**C**) Double staining for F-actin and protocadherin 15 in the organ of Corti. (A) Rhodamine-phalloidin staining in stereocilia of cochlear inner hair cells and three rows of outer hair cells (red channel). (B) Protocadherin 15 was detected using rabbit anti-Pcdh15 antiserum (PB303) in stereocilia of inner and outer hair cells (green channel). (C) Double staining for protocadherin 15 and F-actin revealed colocalization of these proteins in stereocilia (red and green channels together). (**D**–**F**) Double staining for protocadherin 15 and F-actin at the level of hair cell cuticular plate. (D) Actin is concentrated at the cuticular plates of hair cells, forming characteristic heart-shape cuticular plates of three rows of outer hair cells. (E) Protocadherin 15 is also concentrated at the cuticular plate level (arrows) and colocalized with actin (F). The region of the pericuticular necklace (arrowheads) around the cuticular plates of inner hair cells is also stained (E, F). In hair cell stereocilia of the ampulla (**G**–**I**) protocadherin 15 was detected along the length of stereocilia and its expression level varied between stereocilia of the same bundles and between different hair bundles. The longer stereocilia usually exhibited brighter staining (H, I). In utricular hair cells (**J**–**L**) the pattern of stereocilia staining with anti-protocadherin 15 antibody was similar to that of ampulla hair cell stereocilia (K, L). The differential staining of the longer (arrows) and shorter (arrowheads) stereocilia are more apparent in utricular hair cells (K, L). Scale bar in (L), 10 μm applied to all panels.

(Molecular Probes, Eugene, OR, USA) and viewed with a LSM510 Zeiss confocal microscope (35).

Immunohistology of human and monkey retina

Human donor eyes were obtained from a Caucasian male (74 years old) who died of congestive heart failure. Tissues were obtained by S.L.B. from the Maryland State Anatomy Board under IRB exemption SB-019701. Eyes were prepared 6 h post-mortem. The anterior segment eye tissues (cornea, iris) and posterior non-retina tissues (lens, vitreous, ciliary body) were removed, and eyes dissected away, and posterior poles fixed in 4% PFA-PBS for 2 h. Tissue was then dehydrated through graded ethanol (70, 80 and 95% and absolute), cleared in xylene, embedded in paraffin, and 6 µm sections collected on superfrost plus slides (Fisher). Following sectioning, slides were deparaffinized in xylene and rehydrated through graded ethanol and PBS. Tissue sections were reacted O/N at 4°C with primary antibody (PB303) at a concentration of ~5 µg/ml in 2% BSA. Treated sections were incubated with alkaline phosphatase secondary antibody (Vector Laboratories, Burlingame, CA, USA). Adolescent monkey eyes (3 years of age) were obtained by S.L.B. from John Cogan (Bureau of Biologics, FDA, Bethesda, MD, USA). Tissue was fixed in 4% PF-PBS and frozen in OCT. Ten micron frozen sections were blocked for 1 h with 5% normal goat serum containing 2% bovine serum albumen. Tissue sections were reacted O/N at 4°C with primary antibody (PB303) at a concentration of ~5 µg/ml containing 2% BSA. Treated sections were incubated with alkaline phosphatase secondary antibody (Vector Laboratories, Burlingame, CA, USA). The slides were not counterstained.

ACKNOWLEDGEMENTS

We thank the families for their participation in this study, which was supported by NIDCD/NIH, Intramural Research fund Z01DC00035-06, Z01DC00039-06 and Z01DC00064-02. Part of this study in Pakistan was supported by Higher Education Commission, Islamabad, Pakistan and by the International Centre for Genetic Engineering and Biotechnology, Trieste, Italy under Project CRP/PAK02-01 (contract no. 02/013). S.L.B. is the recipient of a career development award (CDA) from Research to Prevent Blindness (RPB-USA), and funded by the V. Kann Rasmussen Foundation (Denmark). We thank Shaheen Khan and Barbara Ploplis for their technical help. We also thank Tomoko Makishima, Rob Morell, Julie Schultz, Tamar Ben-Yosuf, Kiyoto Kurima, Ayala Lagziel, Doris Wu and Dennis Drayna for advice and comments in preparing the manuscript.

REFERENCES

1. Smith, R.J., Berlin, C.I., Hejtmancik, J.F., Keats, B.J., Kimberling, W.J., Lewis, R.A., Moller, C.G., Pelias, M.Z. and Tranebjaerg, L. (1994) Clinical diagnosis of the Usher syndromes. Usher Syndrome Consortium. *Am. J. Med. Genet.*, **50**, 32–38.
2. Ahmed, Z., Riazuddin, S. and Wilcox, E. (2003) The molecular genetics of Usher syndrome. *Clin. Genet.*, **63**, 431–444.
3. Ahmed, Z.M., Riazuddin, S., Bernstein, S.L., Ahmed, Z., Khan, S., Griffith, A.J., Morell, R.J., Friedman, T.B. and Wilcox, E.R. (2001) Mutations of the protocadherin gene PCDH15 cause Usher syndrome type 1F. *Am. J. Hum. Genet.*, **69**, 25–34.
4. Alagramam, K.N., Yuan, H., Kuehn, M.H., Murcia, C.L., Wayne, S., Srisailpathy, C.R., Lowry, R.B., Knaus, R., Van Laer, L., Bernier, F.P. *et al.* (2001) Mutations in the novel protocadherin PCDH15 cause Usher syndrome type 1F. *Hum. Mol. Genet.*, **10**, 1709–1718.
5. Bolz, H., von Brederlow, B., Ramirez, A., Bryda, E.C., Kutsche, K., Nothwang, H.G., Seeliger, M., del, C.S.C.M., Vila, M.C., Molina, O.P. *et al.* (2001) Mutation of CDH23, encoding a new member of the cadherin gene family, causes Usher syndrome type 1D. *Nat. Genet.*, **27**, 108–112.
6. Bork, J.M., Peters, L.M., Riazuddin, S., Bernstein, S.L., Ahmed, Z.M., Ness, S.L., Polomeno, R., Ramesh, A., Schloss, M., Srisailpathy, C.R. *et al.* (2001) Usher syndrome 1D and nonsyndromic autosomal recessive deafness DFNB12 are caused by allelic mutations of the novel cadherin-like gene CDH23. *Am. J. Hum. Genet.*, **68**, 26–37.
7. Bitner-Glindzicz, M., Lindley, K.J., Rutland, P., Blaydon, D., Smith, V.V., Milla, P.J., Hussain, K., Furth-Lavi, J., Cosgrove, K.E., Shepherd, R.M. *et al.* (2000) A recessive contiguous gene deletion causing infantile hyperinsulinism, enteropathy and deafness identifies the Usher type 1C gene. *Nat. Genet.*, **26**, 56–60.
8. Verpy, E., Leibovici, M., Zwaenepoel, I., Liu, X.Z., Gal, A., Salem, N., Mansour, A., Blanchard, S., Kobayashi, I., Keats, B.J. *et al.* (2000) A defect in harmonin, a PDZ domain-containing protein expressed in the inner ear sensory hair cells, underlies Usher syndrome type 1C. *Nat. Genet.*, **26**, 51–55.
9. Weil, D., El-Amraoui, A., Masmoudi, S., Mustapha, M., Kikkawa, Y., Laine, S., Delmaghani, S., Adato, A., Nadifi, S., Zina, Z.B. *et al.* (2003) Usher syndrome type I G (USH1G) is caused by mutations in the gene encoding SANS, a protein that associates with the USH1C protein, harmonin. *Hum. Mol. Genet.*, **12**, 463–471.
10. Weil, D., Blanchard, S., Kaplan, J., Guilford, P., Gibson, F., Walsh, J., Mburu, P., Varela, A., Levilliers, J., Weston, M.D. *et al.* (1995) Defective myosin VIIA gene responsible for Usher syndrome type 1B. *Nature*, **374**, 60–61.
11. Ahmed, Z.M., Smith, T.N., Riazuddin, S., Makishima, T., Ghosh, M., Bokhari, S., Menon, P.S.N., Desmukh, D., Griffith, A.J., Riazuddin, S. *et al.* (2002) Nonsyndromic recessive deafness *DFNB18* and Usher syndrome type IC are allelic mutations of *USH1C.Hum. Genet.*, **72**, 1315–1322.
12. Ouyang, X.M., Xia, X.J., Verpy, E., Du, L.L., Pandya, A., Petit, C., Balkany, T., Nance, W.E. and Liu, X.Z. (2002) Mutations in the alternatively spliced exons of USH1C cause non-syndromic recessive deafness. *Hum. Genet.*, **111**, 26–30.
13. Ben-Yosef, T., Ness, S.L., Madeo, A.C., Bar-Lev, A., Wolfman, J.H., Ahmed, Z.M., Desnick, R.J., Willner, J.P., Avraham, K.B., Ostrer, H. *et al.* (2003) A mutation of PCDH15 among Ashkenazi Jews with the type 1 Usher syndrome. *New Engl. J. Med.*, **348**, 1664–1670.
14. Angst, B.D., Marcozzi, C. and Magee, A.I. (2001) The cadherin superfamily: diversity in form and function. *J. Cell Sci.*, **114**, 629–641.
15. Suzuki, S.T. (2000) Recent progress in protocadherin research. *Exp. Cell Res.*, **261**, 13–18.
16. Alagramam, K.N., Murcia, C.L., Kwon, H.Y., Pawlowski, K.S., Wright, C.G. and Woychik, R.P. (2001) The mouse Ames waltzer hearing-loss mutant is caused by mutation of Pcdh15, a novel protocadherin gene. *Nat. Genet.*, **27**, 99–102.
17. Raphael, Y., Kobayashi, K.N., Dootz, G.A., Beyer, L.A., Dolan, D.F. and Burmeister, M. (2001) Severe vestibular and auditory impairment in three alleles of Ames waltzer (av) mice. *Hear. Res.*, **151**, 237–249.
18. Schaible, R.H. (1961) Ames Waltzer, av. *Mouse News Lett.*, **24**, 38.
19. Schaible, R.H. (1956) av. *Mouse News Lett.*, **15**, 29.
20. Gibson, F., Walsh, J., Mburu, P., Varela, A., Brown, K.A., Antonio, M., Beisel, K.W., Steel, K.P. and Brown, S.D. (1995) A type VII myosin encoded by the mouse deafness gene shaker-1. *Nature*, **374**, 62–64.
21. Di Palma, F., Holme, R.H., Bryda, E.C., Belyantseva, I.A., Pellegrino, R., Kachar, B., Steel, K.P. and Noben-Trauth, K. (2001) Mutations in Cdh23, encoding a new type of cadherin, cause stereocilia disorganization in waltzer, the mouse model for Usher syndrome type 1D. *Nat. Genet.*, **27**, 103–107.
22. Kikkawa, Y., Shitara, H., Wakana, S., Kohara, Y., Takada, T., Okamoto, M., Taya, C., Kamiya, K., Yoshikawa, Y., Tokano, H. *et al.* (2003) Mutations in a new scaffold protein Sans cause deafness in Jackson shaker mice. *Hum. Mol. Genet.*, **12**, 453–461.

23. Boeda, B., El-Amraoui, A., Bahloul, A., Goodyear, R., Daviet, L., Blanchard, S., Perfettini, I., Fath, K.R., Shorte, S., Reiners, J. *et al.* (2002) Myosin VIIa, harmonin and cadherin 23, three Usher I gene products that cooperate to shape the sensory hair cell bundle. *EMBO J.*, **21**, 6689–6699.
24. Siemens, J., Kazmierczak, P., Reynolds, A., Sticker, M., Littlewood-Evans, A. and Muller, U. (2002) The Usher syndrome proteins cadherin 23 and harmonin form a complex by means of PDZ-domain interactions. *Proc. Natl Acad. Sci. USA*, **99**, 14946–14951.
25. Hasson, T., Heintzelman, M.B., Santos-Sacchi, J., Corey, D.P. and Mooseker, M.S. (1995) Expression in cochlea and retina of myosin VIIa, the gene product defective in Usher syndrome type 1B. *Proc. Natl Acad. Sci. USA*, **92**, 9815–9819.
26. Liu, X., Vansant, G., Udovichenko, I.P., Wolfrum, U. and Williams, D.S. (1997) Myosin VIIa, the product of the Usher 1B syndrome gene, is concentrated in the connecting cilia of photoreceptor cells. *Cell Motil. Cytoskeleton*, **37**, 240–252.
27. Wolfrum, U. and Schmitt, A. (2000) Rhodopsin transport in the membrane of the connecting cilium of mammalian photoreceptor cells. *Cell Motil. Cytoskeleton*, **46**, 95–107.
28. Astuto, L.M., Bork, J.M., Weston, M.D., Askew, J.W., Fields, R.R., Orten, D.J., Ohliger, S.J., Riazuddin, S., Morell, R.J., Khan, S. *et al.* (2002) CDH23 mutation and phenotype heterogeneity: a profile of 107 diverse families with Usher syndrome and nonsyndromic deafness. *Am. J. Hum. Genet.*, **71**, 262–275.
29. Pickles, J.O., Comis, S.D. and Osborne, M.P. (1984) Cross-links between stereocilia in the guinea pig organ of Corti, and their possible relation to sensory transduction. *Hear. Res.*, **15**, 103–112.
30. Tsuprun, V. and Santi, P. (2002) Structure of outer hair cell stereocilia side and attachment links in the chinchilla cochlea. *J. Histochem. Cytochem.*, **50**, 493–502.
31. Pujol, R., Lavigne-Rebillard, M. and Lenoir, M. (1997) Development of sensory and neural structures in the mammalian cochlea. In: Rubel, E.W., Popper, A.N. and Fay, R.R. (eds.), *Development of the Auditory System*, 9th edn. Springer, New York, Vol. 1, pp. 146–192.
32. Goodyear, R. and Richardson, G. (1992) Distribution of the 275 kD hair cell antigen and cell surface specialisations on auditory and vestibular hair bundles in the chicken inner ear. *J. Comp. Neurol.*, **325**, 243–256.
33. Goodyear, R.J., Marcotti, W., Kros, C.J. and Richardson, G.P. (2003) In: Santi, P.A. (ed.), *Development of Hair-Bundle Specialization in Outer Hair Cells of the Postnatal Mouse Cochlea.* Association for Research in Otolaryngology, Daytona Beach, FL, Vol. 26, p. 122.
34. Schaffer, A.A. (1996) Faster linkage analysis computations for pedigrees with loops or unused alleles. *Hum. Hered.*, **46**, 226–235.
35. Belyantseva, I.A., Adler, H.J., Curi, R., Frolenkov, G.I. and Kachar, B. (2000) Expression and localization of prestin and the sugar transporter GLUT-5 during development of electromotility in cochlear outer hair cells. *J. Neurosci.*, **20**, RC116.
36. Ball, S.L., Bardenstein, D. and Alagramam, K.N. (2003) Assessment of retinal structure and function in Ames waltzer mice. *Invest. Ophthalmol. Vis. Sci.*, **44**, 3986–3992.